water

MDPI

Article

Backwater Effect of Clogging of Aquatic Plants at Fine-Particle Screens on Inland Flooding in Okayama

Takumi Inaba *, Kumiko Tsujimoto * and Yoshitaka Nakashima

Graduate School of Environmental and Life Science, Okayama University, Okayama 700-8530, Japan; nakayosi@cc.okayama-u.ac.jp

* Correspondence: pnsd9rkb@s.okayama-u.ac.jp (T.I.); tsujimoto@okayama-u.ac.jp (K.T.); Tel./Fax: +81-86-251-8874 (T.I. & K.T.)

Abstract: In low-lying Okayama city, Japan, the heavy rainfall frequency and intensity have recently increased, subjecting the city to inland flooding. Another factor increasing the inland flooding risk is fine-particle screen clogging by aquatic plants at drainage pump stations, which obstructs drainage and causes backwater. In this study, water level simulations were conducted in drainage pump station channels to clarify the inland flooding risks with and without aquatic plant clogging-induced backwater at fine-particle screens. In the Urayasu West Drainage Pump Station channels, without backwater, no inland flooding occurred under an initial water level of 70% of the channel depth and a 40 m^3/s discharge. However, when backwater deeper than 0.2 m occurred under the same conditions, inland flooding occurred, indicating an increased inland flooding risk associated with backwater. Additionally, we conducted an aquatic plant distribution survey in the main Okayama city channels and proposed six priority control sections based on sections with thriving aquatic plants. Although no previous inland flooding studies have considered aquatic plant clogging-induced backwater at fine-particle screens, aquatic plants cause clogging problems and drainage obstructions at water control facilities worldwide. Therefore, this study reveals the importance of conducting water level simulations and distribution surveys in areas other than Okayama city.

Keywords: fragments of aquatic plants; fine-particle screens; inland flooding

Citation: Inaba, T.; Tsujimoto, K.; Nakashima, Y. Backwater Effect of Clogging of Aquatic Plants at Fine-Particle Screens on Inland Flooding in Okayama. *Water* **2022**, *14*, 1980. https://doi.org/10.3390/w14131980

Academic Editors: Agnieszka Pociecha, Henri J. Dumont and Joanna Czerwik-Marcinkowska

Received: 13 May 2022
Accepted: 13 June 2022
Published: 21 June 2022

1. Introduction

According to the Sixth Report of the Intergovernmental Panel on Climate Change (IPCC), the average amount of precipitation that falls over land is likely to have increased globally since the 1950s, and the rate of increase has accelerated since the 1980s. The frequency and intensity of heavy rainfall have been increasing since the 1950s, and anthropogenic climate change is likely the main driver of this increase; as global warming progresses, heavy rainfall is likely to become more intense and frequent in many areas [1]. In this way, extreme rainfall is increasing due to climate change.

The frequency of heavy rainfall is also increasing in Japan. According to the Japan Meteorological Agency, Tokyo, Japan [2], the number of annual occurrences of precipitation events of 50 mm or more per hour (statistical period: 1976–2020) has been increasing in Japan, and the average number of these annual occurrences measured between 2011–2020, approximately 334, was approximately 1.5 times higher than that measured between 1976–1985, which was approximately 226. These changes will increase the risk of inland flooding in the future.

Inland flooding occurs when heavy rain falls on flat land and causes the water levels of channels and small rivers to rise. Flat land is difficult to drain because of its low-angle slopes, so the water level rises, and channels easily overflow. Landforms that are prone to inland flooding include highly urbanized areas, subsidence areas, low-lying areas, and reclaimed lands [3]. Many cities in Japan are located in low-lying areas, downstream of

major rivers, and the damage caused by inland flooding is increasing due to factors such as the expansion of impervious areas as a result of significant urbanization in recent years and the increase in torrential rains [4]. This situation also applies to Okayama city in western Japan, the target site of this study.

Okayama city is located on the Okayama Plain, a vast low-lying area in which the urban area is lower than the levels of nearby rivers, making it difficult to drain water from the city during heavy rainfall. Okayama city has been flooded many times due to this topographical feature. During the 10-year period from 2007–2016, inundation damage occurred 30 times, and 98% of the total damage was caused by inland flooding [5]. Thus, Okayama city is particularly prone to inland flooding.

Another factor that increases the risk of inland flooding in Okayama city is the problem of aquatic plant growth. In recent years, a large number of aquatic plants have grown densely in local channels, blocking the flow of water [6]. During heavy rains, aquatic plant fragments clog the fine-particle screens in the Urayasu area located in the southern part of Okayama city, obstructing the flow of water draining through the screens. Due to these clogging fragments of aquatic plants, the water level of the channels rises at the screens, and backwater develops, leading to inland flooding in the areas surrounding the screens. In this way, aquatic plants are closely related to inland flooding. Because some species of aquatic plants easily accumulate in fine-particle screens in Okayama city while other species rarely accumulate in the screens, we believe that the total volume of clogging plants could be efficiently reduced by strategically controlling the easily accumulating species. The main plants that accumulate in fine-particle screens consist of five species: *Egeria densa*, *Elodea nuttallii*, *Hydrilla verticillata*, *Lagarosiphon major*, and *Vallisneria asiatica*. Therefore, these five species should be specifically controlled.

Various effects of aquatic plants on flood control have been reported worldwide. For example, in Lake Inba in Chiba Prefecture, an aquatic plant called *Alternanthera philoxeroides* has thrived in the entire basin and has invaded not only lakes and rivers but also drainage channels and drainage pump stations, thus interfering with the water flow and drainage processes. At drainage pump stations, the large amounts of *A. philoxeroides* that drift ashore when the pumps are in operation have become a flood control problem, and a great deal of labor and money has been required to dispose of this species [7]. Overseas, for example, *Eichornia crassipes* causes clogging in channels, sewers, and sewer pipes in the USA [8]. In Bangladesh, aquatic vegetation clogs gates, siphons, and pumps, thus blocking the flow of water in irrigation systems and drainage channels [9]. Afrozah Hassan and Nawchoo [10] reported that the extreme growth of aquatic plants can lead to flooding because the growing plants can block channels and subsequently reduce the water flow. Narayan et al. [11] reported that excessive plant propagation leads to silt deposition and reduced water flows in rivers, channels, lakes, and reservoirs, subsequently leading to flooding and bank erosion and hindering recreation. Bornette et al. [12] studied the effects of connectivity between cutoff channels and a river on aquatic plant diversity or rarity and reported that the most frequently flooded channels showed the highest species richness and the occurrence of rare and escaped species.

In one study performed in a low-lying area similar to Okayama city, Kawaike et al. [13] analyzed inland flooding in the Neyagawa River basin in Osaka Prefecture. They developed a numerical model to represent the complex behavior of inundation water by integrating four submodels: a mountainous area submodel, a river network submodel, a sewer network submodel, and an inland area submodel. In their analysis results, the authors confirmed that areas with lower ground levels relative to the surrounding areas, river embankments, and areas along the railroad embankments were more likely to collect flood waters and were thus the more dangerous areas with regard to flooding. In a study by Sekine [14] on internal flooding in central Tokyo, a street network flooding and inundation analysis model was constructed. The model was characterized by modeling the process by which rainwater falls on residential roofs and flows into the sewage system, which had not been previously considered, and by analyzing the flow of urban rivers in a realistic manner.

Djamres et al. [15] conducted statistical analysis and geographic information system (GIS) calculations for Tangerang city, Indonesia, where frequent inland flooding has occurred. In their study, they used inland flooding records and a digital elevation model (DEM) obtained from the government to extract the topographical features of frequently flooded areas in Tangerang city and identify the main characteristics of these areas.

Although many studies have been conducted on inland flooding, Nakaguchi et al. [16], who categorized the causes of inland flooding into meteorological, topographical, and urban factors based on the results of previous studies, pointed out that the relationships between the city size or internal flooding risk and various risk factors have not yet been quantitatively evaluated, as previous studies focused on specific areas or single factors.

While aquatic vegetation has an impact on inland flooding, this risk factor has not been examined in detail in published research. In addition, previous studies have considered the effects of topography and sewage systems on inland flooding but have not considered the effects of backwater at the ends of channels due to clogging by aquatic plant fragments in fine-particle screens and other equipment.

In this study, we conducted hydraulic water level simulations in the main channels in Okayama city to consider the effects of backwater due to the clogging of fine-particle screens by aquatic plants, thus simulating how clogging alters the water level and overflow risk. In addition, we investigated the distribution of the aquatic plant species that tend to accumulate on fine-particle screens to strategically identify sections for priority control.

2. Materials and Methods

2.1. Target Channels and Watershed

Figure 1 shows the location of Okayama city, the channels targeted in this study and the watershed comprising all target channels. These channels mainly include the main channels in Okayama city that flow from the water intake station at Mino to the Urayasu East and Urayasu West Drainage Pump Stations. Because these main channels do not flow directly into the Urayasu West Drainage Pump Station, the nonmain channel that flows in front of the pump station was selected for analysis in this study.

The watershed comprising all target channels was first determined based on the topography data and the watersheds of the surrounding rivers. Then, the watershed area containing all target channels was assigned based on the widths of the four outlets, including the Urayasu East and Urayasu West Drainage Pump Station channels. Figure 2 shows the outlet locations. Table 1 shows the channel width at each outlet, and Table 2 shows the areas of the watersheds corresponding to the target channels and the channels of each drainage pump station.

Table 1. Channel width at each outlet.

	Urayasu East Drainage Pump Station	Urayasu West Drainage Pump Station	Aioi River	Konan Pump Station
Channel width [m]	13	11	20	13

Table 2. Areas of the watershed containing all target channels and of the watersheds corresponding to the four outlet channels.

	Entire Target Channels	Urayasu East Drainage Pump Station	Urayasu West Drainage Pump Station	Aioi River	Konan Pump Station
Area of watershed [m2]	2.7×10^7	6.2×10^6	5.2×10^6	9.4×10^6	6.2×10^6

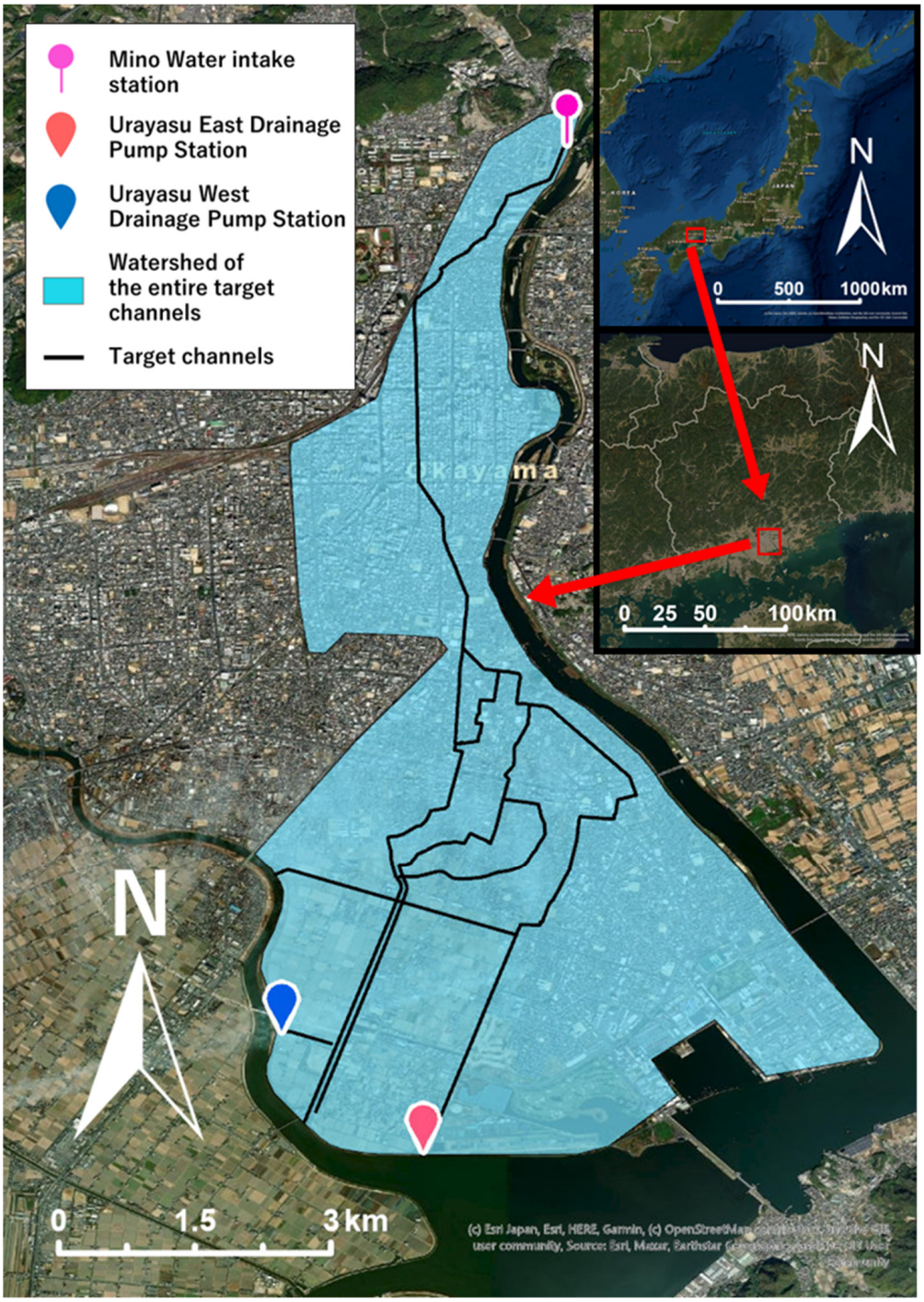

Figure 1. Target channels analyzed in this study and watershed containing all target channels (the red arrows mean that the figures in the red frames are enlarged). Copyright: Esri Japan, Esri, HERE, Garmin; OpenStreetMap contributors, and the GIS user community. Source: Esri, Maxar, Earthstar Geographics, and the GIS user community.

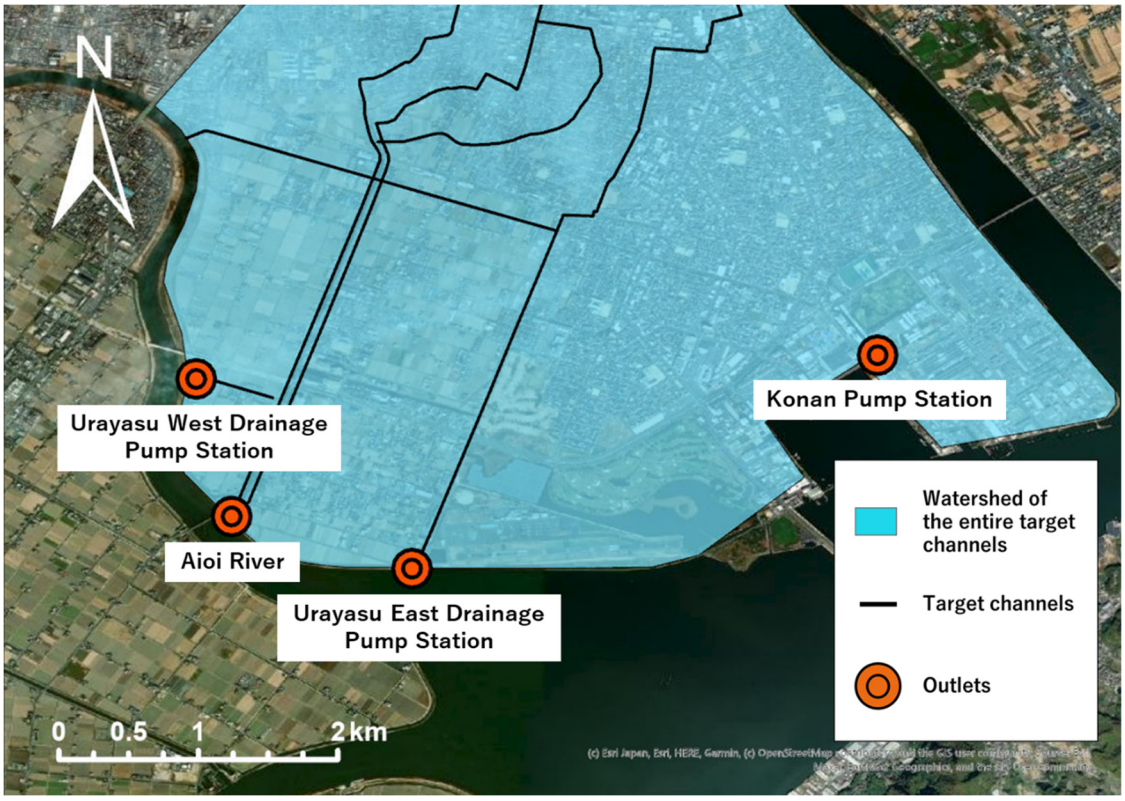

Figure 2. Location of each outlet. Copyright Esri Japan, Esri, HERE, Garmin; OpenStreetMap contributors, and the GIS user community. Source: Esri, Maxar, Earthstar Geographics, and the GIS user community.

2.2. Water Level Simulation

2.2.1. Channel Structure Investigation

The width, bed height, and Manning's roughness coefficient of each channel were investigated, as these are necessary data for water level simulations. Regarding the channel width, measurements were taken at locations where the width clearly changed. At points where the channel width could not be measured due to excessive width, the width was measured on a map using GIS software (ArcGIS Pro 2.5.0, Esri Inc., Redlands, CA, USA). The channel bed height was surveyed at the same measurement points as the channel widths. The elevations of the measurement points were obtained from the 5-m mesh data constructing the DEM published by the Geospatial Information Authority of Japan (https://fgd.gsi.go.jp/download/menu.php, accessed on 18 May 2021). The channel bed elevation was calculated by subtracting the depth of the channel measured at each point from the corresponding elevation. The Manning's roughness coefficients were obtained from the Ministry of Land, Infrastructure, Transport and Tourism [17] after assessing the composition of the material in each analyzed channel.

The channel structures used in the water level simulations were created using the channel structure survey results and data obtained using GIS software. Figure 3 and Table 3 provide a map of and information on the Urayasu East Drainage Pump Station channel structure, respectively, and Figure 4 and Table 4 show the characteristics of the Urayasu West Drainage Pump Station channel structure. The numbers in the channels indicate the cross-section number, and these cross-section locations correspond to channel structure changes. The elevations of the left and right banks at each point were obtained from the DEM. If the water level at a given cross-section rose above the elevation of the left or right bank, inland flooding was considered to occur at the bank.

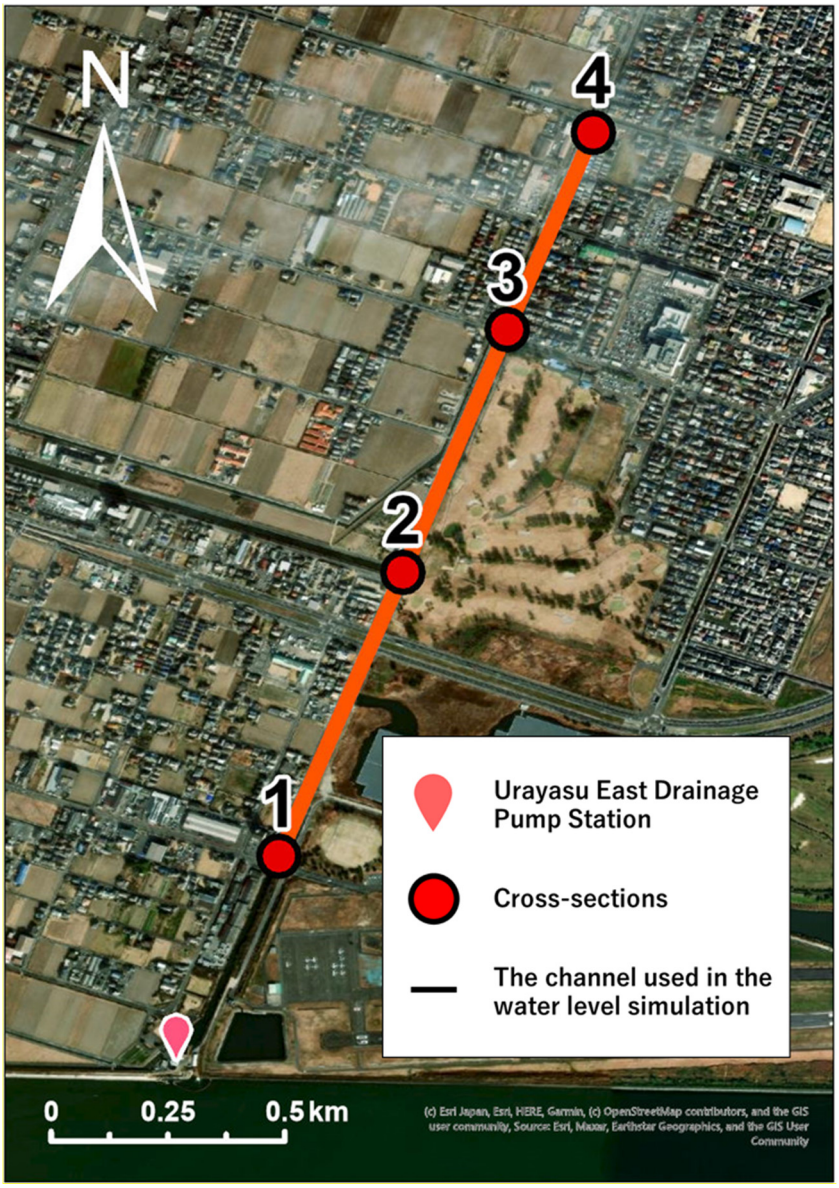

Figure 3. Urayasu East Drainage Pump Station channel map. Cross-sections were used when points to change parameters as the channel structure changes. Copyright: Esri Japan, Esri, HERE, Garmin; OpenStreetMap contributors, and the GIS user community. Source: Esri, Maxar, Earthstar Geographics, and the GIS user community.

Table 3. Channel structure of the Urayasu East Drainage Pump Station.

	Distance between Cross Sections [m]	Channel Width [m]	Distance from Measurement Points to Channel Bed [m]	Right Bank Elevation [m]	Left Bank Elevation [m]	Channel Bed Height [m]	Channel Bed Gradient	Manning's Roughness Coefficient [$m^{-1/3} \cdot s$] *
Cross section 1			2.7	−0.2	−0.5	−3.2		
	647.8	13.4					9.3×10^{-4}	1.7×10^{-2}
Cross section 2			3.2	0.6	0.3	−2.6		
	538.9	9.4					5.6×10^{-4}	1.7×10^{-2}
Cross section 3			2.3	0	0.3	−2.3		
	457.1	7.4					6.6×10^{-4}	1.7×10^{-2}
Cross section 4			1.9	0	−0.1	−2.0		

* The Manning's roughness coefficients were obtained from the Ministry of Land, Infrastructure, Transport and Tourism [17].

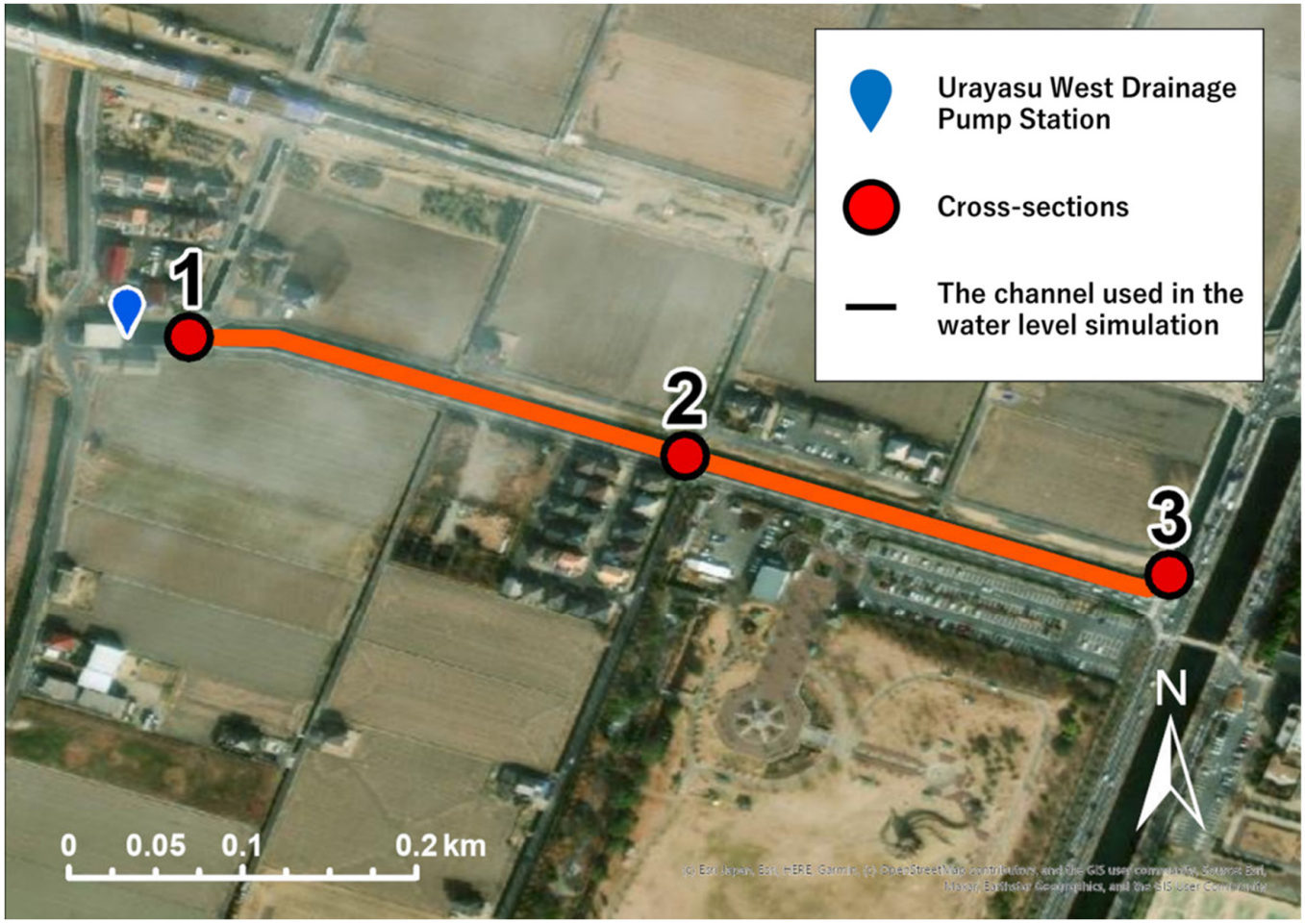

Figure 4. Urayasu West Drainage Pump Station channel map. Cross-sections were used when points to change parameters as the channel structure changes. Copyright: Esri Japan, Esri, HERE, Garmin; OpenStreetMap contributors, and the GIS user community. Source: Esri, Maxar, Earthstar Geographics, and the GIS user community.

Table 4. Channel structure of the Urayasu West Drainage Pump Station.

	Distance between Cross Sections [m]	Channel Width [m]	Distance from Measurement Points to Channel Bed [m]	Right Bank Elevation [m]	Left Bank Elevation [m]	Channel Bed Height [m]	Channel Bed Gradient	Manning's Roughness Coefficient [$m^{-1/3} \cdot s$] *
Cross section 1			2.4	−0.2	−0.2	−2.6		
	234.7	11.1					8.5×10^{-4}	1.7×10^{-2}
Cross section 2			2.1	−0.4	−0.3	−2.4		
	248.6	8.1					4.0×10^{-4}	1.7×10^{-2}
Cross section 3			1.9	0.4	−0.4	−2.3		

* The Manning's roughness coefficients were obtained from the Ministry of Land, Infrastructure, Transport and Tourism [17].

2.2.2. Equation Used in the Water Level Simulations

The following equation (Equation (1)) for varied flow [18] was used in the simulations performed in this study. This equation implies that the energy conservation law is valid for both the upstream and downstream sides. We considered the subcritical flow, so the water level calculation was performed from the downstream direction to the upstream direction,

and the water level was calculated by differentiating the channels between each section into 10 equal parts:

$$z_2 + h_2 + \frac{Q^2}{2gB_2^2h_2^2} + \frac{n^2Q^2\Delta x}{2B_2^2h_2^{\frac{10}{3}}} = z_1 + h_1 + \frac{Q^2}{2gB_1^2h_1^2} - \frac{n^2Q^2\Delta x}{2B_1^2h_1^{\frac{10}{3}}} \quad (1)$$

where Q is the discharge (m^3/s), H is the water level (m), z is the channel bed height (m), h is the water depth, B is the channel width (m), and Δx is the distance between the differentiated cross-sections (m). Subscripts 1 and 2 refer to the values at the upstream and downstream ends, respectively.

The velocity of flow was obtained under the assumption of uniform conditions by the Manning's equation with the bed gradient and the Manning's roughness coefficient of each cross-section of the channel.

2.2.3. Setting of Parameters

We simulated several cases with different initial water depths at the downstream end and different channel discharges. The initial water depths at the downstream end were set to 70%, 50%, and 30% of the channel depth. For each run with a different initial water depth, channel discharges were set in a range from the discharge corresponding to the initial water depth to the discharge corresponding to the 90% channel-depth water level.

In addition, we assumed that there were aquatic plants clogging the screens at the end of the channels in our simulations, with backwater heights of 0.2, 0.4, and 0.6 m in our simulations. This height was added to the initial water depth at the downstream end to conduct the simulations with aquatic plants. We used these backwater heights as predictions because there were no data on how high backwater actually occurs due to clogging by aquatic plants in fine-particle screens.

The frictional losses caused by aquatic plant communities in channels normally inhibit the flow of water and reduce the flow velocity, thus causing the water level to rise. However, because sufficient information for quantitatively estimating frictional energy losses under various community conditions is not available, the effect of frictional losses resulting from the presence of plant communities was not considered in this work.

2.3. Aquatic Plant Distribution Survey Method

The method used to conduct the aquatic plant distribution survey is shown in Figure 5. First, the channels were divided into sections using the points at which the plant community species, number of aquatic plants, or bottom sediment types varied. Then, the vegetation coverage was surveyed within each of these separate sections. The coverage is the area of the aboveground portion of a grass species relative to the ground surface; this value is expressed as a percentage [19]. In this distribution survey, coverage was considered to represent the area of aquatic vegetation covering each channel. The coverage of each aquatic plant species growing in each section was visually calculated and recorded through degree classification according to Penfound's method [18]. In this method, the vegetation coverage was classified into 6 categories: 4 for 100–76%, 3 for 75–51%, 2 for 50–26%, 1 for 25–6%, 1′ for 5–1%, and + for less than 1%. In this study, a grade of "0" was added to represent areas in which no aquatic plants were found, and areas that could not be surveyed were designated "not surveyable". The survey results were visualized using maps constructed by GIS software.

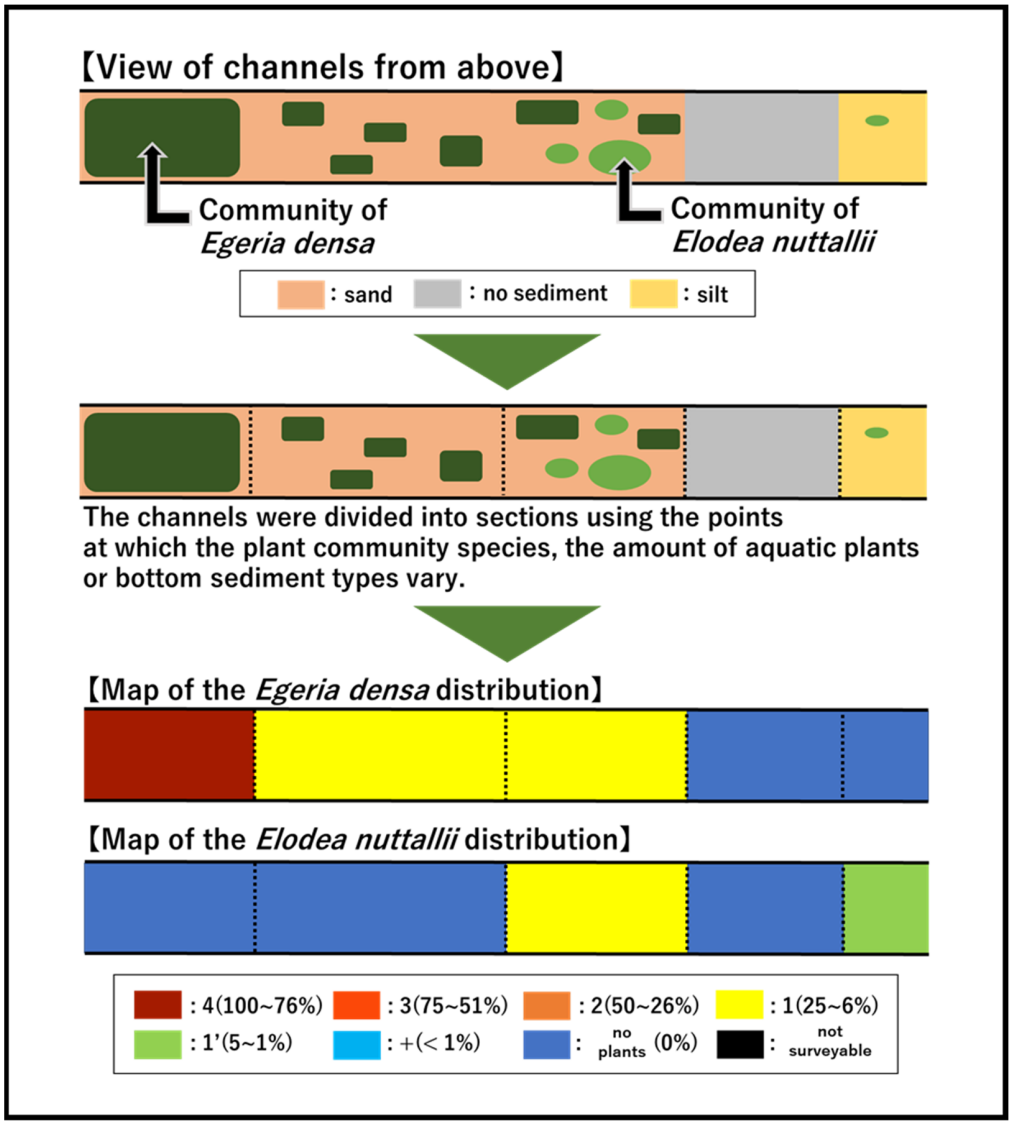

Figure 5. Aquatic plant distribution survey methodology.

3. Results and Discussion

3.1. Water Level Simulation Results

Tables 5 and 6 and Figures 6 and 7 show the water level simulation results. The hatched cells in Tables 5 and 6 indicate the locations where inland flooding occurs, with numbers indicating the cross-section numbers and "R" and "L" indicating the left and right banks, respectively. For example, if inland flooding occurs on the right bank in cross-section 3, this flood is expressed in the table as "3 R". The "-" symbol indicates that the target discharge is exceeded at the initial water depth and thus is not subject to the water level calculation. Blank cells indicate cases in which no inland flooding occurs. For cases where the water level is equal to the elevation of the cross-section bank, the cells are indicated with the "()" symbol. The vertical lines in the graphs in Figures 6 and 7, which indicate the derived water levels, correspond to the locations of the channel cross-sections. When the elevation indicated by the graph is higher than the elevation of the right or left cross-section bank, inland flooding is determined to occur on the bank below the cross-section water level. The locations at which inland flooding newly occurs but backwater does not previously occur are shown with red hatches and red characters. In the figures, only cases with water levels higher than the bank elevation are shown.

Table 5. Water level simulation results obtained for the Urayasu East Drainage Pump Station channel. The hatched cells indicate the locations where inland flooding occurs. The numbers in the columns indicate the cross-sections in which inland flooding occurred, and "R" and "L" indicate the left and right banks, respectively. For cases where the water level is equal to the elevation of the cross-section bank, the cells are indicated with the "()" symbol.

	No Backwater			Backwater Height of 0.2 m			Backwater Height of 0.4 m			Backwater Height of 0.6 m		
	30% of the Channel Depth [13.9 m^3/s]	**50% of the Channel Depth [31.1 m^3/s]**	**70% of the Channel Depth [52.1 m^3/s]**	**30% of the Channel Depth [13.9 m^3/s]**	**50% of the Channel Depth [31.1 m^3/s]**	**70% of the Channel Depth [52.1 m^3/s]**	**30% of the Channel Depth [13.9 m^3/s]**	**50% of the Channel Depth [31.1 m^3/s]**	**70% of the Channel Depth [52.1 m^3/s]**	**30% of the Channel Depth [13.9 m^3/s]**	**50% of the Channel Depth [31.1 m^3/s]**	**70% of the Channel Depth [52.1 m^3/s]**
20 m^3/s [38% of the channel depth]	(4L)	-	-	(4L)	-	-	(4L)	-	-	(4L)	-	-
30 m^3/s [49% of the channel depth]	3R (3L) 4R & L	-	-	3R (3L) 4R & L	-	-	3R (3L) 4R & L	-	-	3R (3L) 4R & L	-	-
40 m^3/s [59% of the channel depth]	3R & L 4R & L	3R & L 4R & L	-	3R & L 4R & L	3R & L 4R & L	-	3R & L 4R & L	3R & L 4R & L	-	3R & L 4R & L	3R & L 4R & L	-
50 m^3/s [68% of the channel depth]	3R & L 4R & L	3R & L 4R & L	-	3R & L 4R & L	3R & L 4R & L	-	3R & L 4R & L	3R & L 4R & L	-	3R & L 4R & L	3R & L 4R & L	-
60 m^3/s [77% of the channel depth]	3R & L 4R & L	3R & L 4R & L	3R & L 4R & L	3R & L 4R & L	3R & L 4R & L	3R & L 4R & L	3R & L 4R & L	3R & L 4R & L	3R & L 4R & L	3R & L 4R & L	3R & L 4R & L	3R & L 4R & L
70 m^3/s [85% of the channel depth]	(2L) 3R & L 4R & L	3R & L 4R & L	3R & L 4R & L	(2L) 3R & L 4R & L	3R & L 4R & L	3R & L 4R & L	(2L) 3R & L 4R & L	3R & L 4R & L	3R & L 4R & L	(2L) 3R & L 4R & L	3R & L 4R & L	3R & L 4R & L

Table 6. Water level simulation results obtained for the Urayasu West Drainage Pump Station channel. The hatched cells indicate the locations where inland flooding occurs. The locations at which inland flooding newly occurs but backwater does not previously occur are shown with red hatches and red characters. The numbers in the columns indicate the cross-sections in which inland flooding occurred, and "R" and "L" indicate the left and right banks, respectively. For cases where the water level is equal to the elevation of the cross-section bank, the cells are indicated with the "()" symbol.

	No Backwater			Backwater Height of 0.2 m			Backwater Height of 0.4 m			Backwater Height of 0.6 m		
	30% of the Channel Depth [8.7 m^3/s]	**50% of the Channel Depth [19.3 m^3/s]**	**70% of the Channel Depth [32.4 m^3/s]**	**30% of the Channel Depth [8.7 m^3/s]**	**50% of the Channel Depth [19.3 m^3/s]**	**70% of the Channel Depth [32.4 m^3/s]**	**30% of the Channel Depth [8.7 m^3/s]**	**50% of the Channel Depth [19.3 m^3/s]**	**70% of the Channel Depth [32.4 m^3/s]**	**30% of the Channel Depth [8.7 m^3/s]**	**50% of the Channel Depth [19.3 m^3/s]**	**70% of the Channel Depth [32.4 m^3/s]**
10 m^3/s [33% of the channel depth]		-	-		-	-		-	-		-	-
20 m^3/s [51% of the channel depth]			-			-			-			-
30 m^3/s [67% of the channel depth]			-			-			-			-
40 m^3/s [81% of the channel depth]	3R	(3R)	(3R)	(3R)	(3R)	3R	(3R)	(3R)	(2R) 3R	(3R)	(3R)	2R (2L) 3R

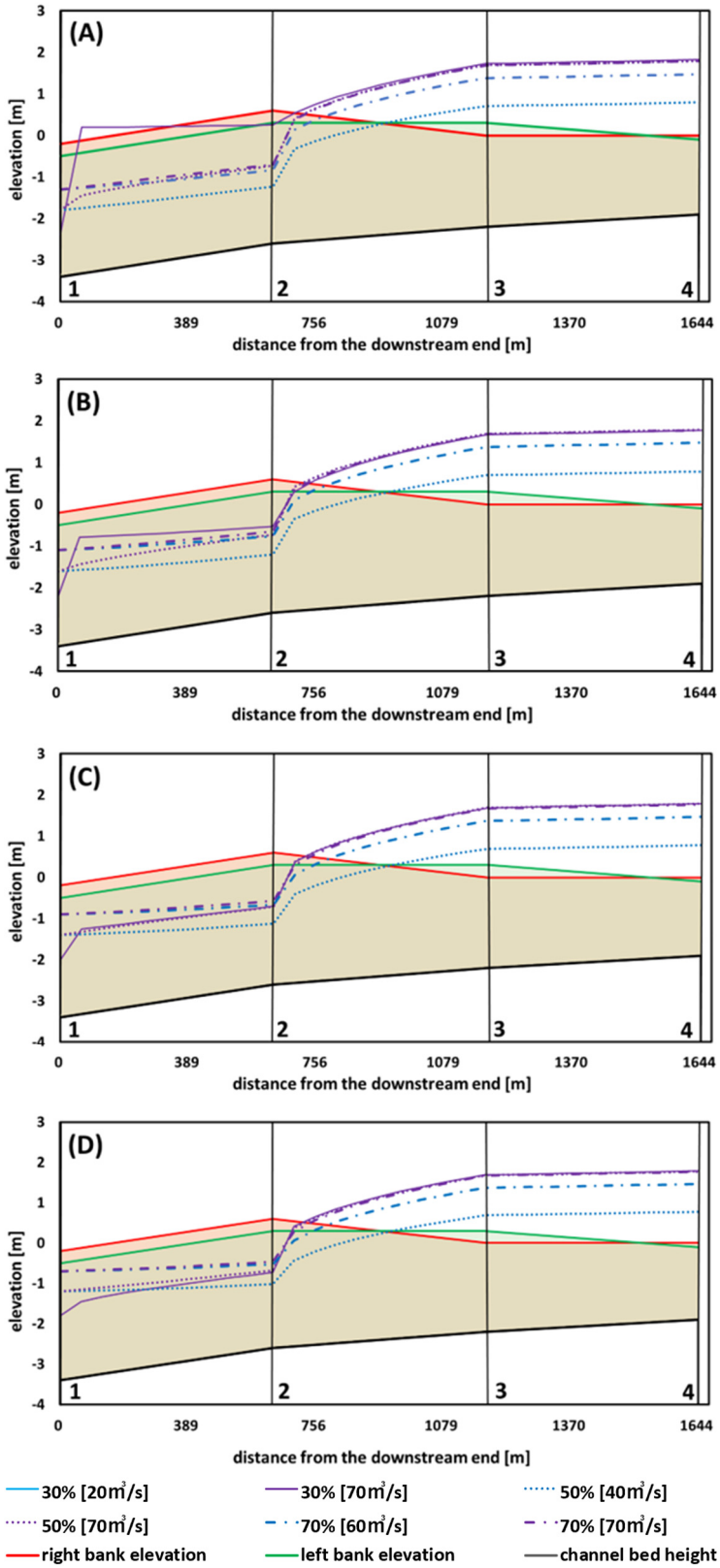

Figure 6. Water level simulation results obtained for the Urayasu East Drainage Pump Station channel ((**A**) no backwater, (**B**) backwater height of 0.2 m, (**C**) backwater height of 0.4 m, (**D**) backwater height of 0.6 m). In the legend, % and [] mean initial water depths and discharges, respectively.

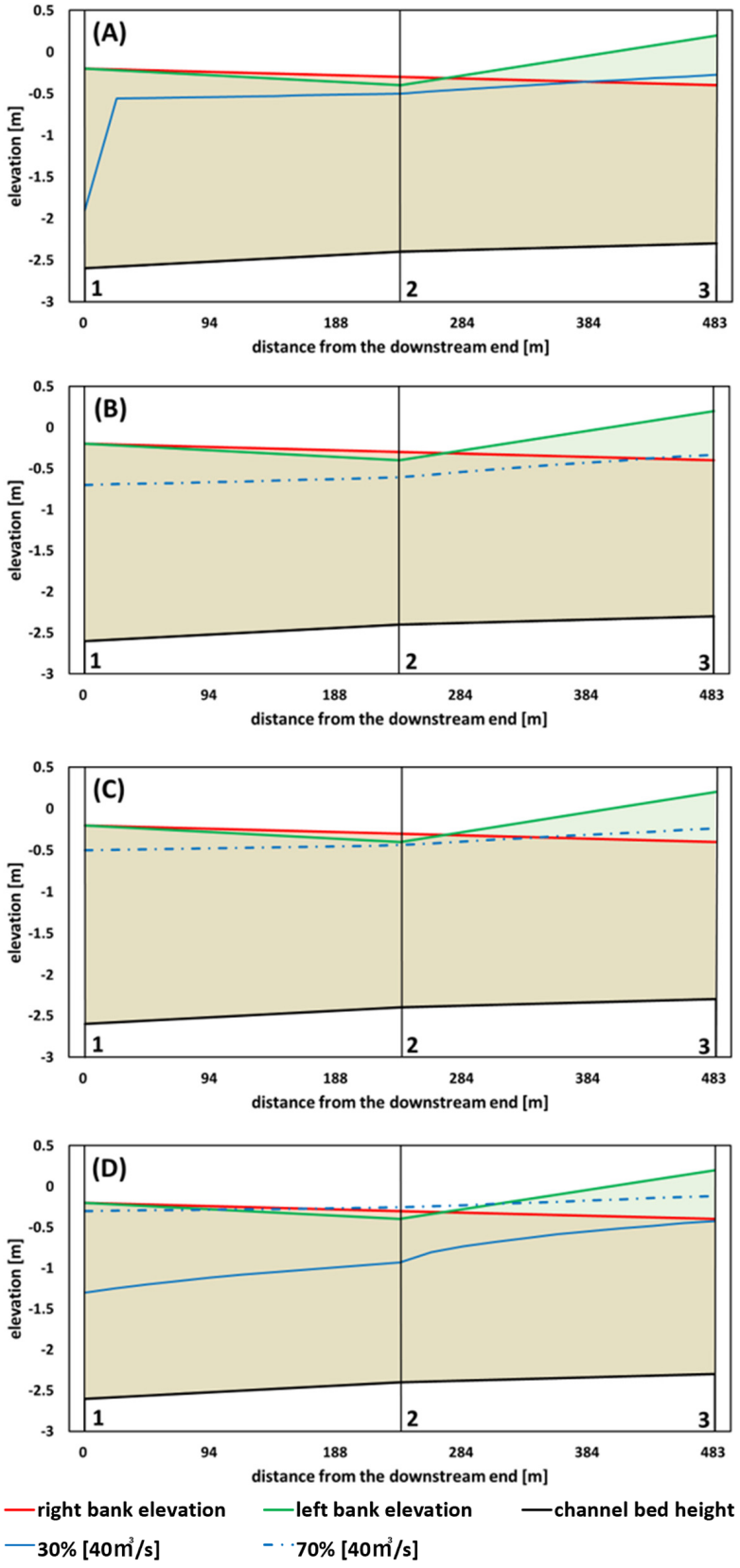

Figure 7. Water level simulation results obtained for the Urayasu West Drainage Pump Station channel ((**A**) no backwater, (**B**) backwater height of 0.2 m, (**C**) backwater height of 0.4 m, (**D**) backwater height of 0.6 m). In the legend, % and [] mean initial water depths and discharges, respectively.

Figure 6 and Table 5 show the results of the Urayasu East Drainage Pump Station channel. In this channel, the locations at which inland flooding occurred with and without backwater were the same for all simulated initial water depths and discharges. Therefore, the increased risk of inland flooding due to backwater is considered to be small in this channel. Although the water level rose sharply after cross-section 2, this was thought to be due to failure to adjust the discharge in consideration of the water channel branch that joins the channel just upstream of cross-section 2.

Figure 7 and Table 6 show the results obtained for the Urayasu West Drainage Pump Station channel. In this channel, when the initial water depths were set to 30% and 50% of the channel depth, the location of inland flooding did not change regardless of whether backwater occurred, except in the case of the 30% initial depth and 40 m^3/s discharge. However, when the backwater height was 0.2 m, inland flooding occurred on the right bank of cross-section 3, and when the backwater height was 0.4 m, the water level was the same as that of the right bank of cross-section 2, and inland flooding occurred on the right bank of cross-section 3. When the backwater height was 0.6 m, inland flooding occurred on the right bank of cross-section 2 and on the right bank of cross-section 3, and the water level was the same height as the left bank of cross-section 2.

These results suggest that when the initial water depth is 70% of the channel depth and the discharge is 40 m^3/s in the Urayasu West Drainage Pump Station channel, inland flooding will not occur unless backwater occurs due to clogging by aquatic plants; however, inland flooding will occur when backwater of 0.2 m or more occurs.

The rainfall intensity corresponding to a discharge of 40 m^3/s is roughly calculated by dividing by the watershed area of the Urayasu West Drainage Pump Station channel, obtaining a rainfall intensity equivalent to 25–30 mm/h. Because this rainfall intensity occurred almost every year over the last five years (2017–2021) in Okayama city [20], the results suggest a risk of inland flooding almost every year that backwater occurs in the Urayasu West Drainage Pump Station channel.

We compared the simulation results with the estimated flooded area due to inland flooding caused by the Heavy Rain Event of July 2018 issued by Okayama city [21]. Since the flooded areas between these two data match fairly well, we adopted the simulation results for the analysis in this study, although further calibration is required for the detailed examination.

3.2. Aquatic Plant Distribution Surveys and Proposed Priority Control Sections

Eight aquatic plant species were identified in the target channels: *E. densa*, *E. nuttallii*, *H. verticillata*, *L. major*, *V. asiatica*, *Potamogeton malaianus*, *Potamogeton maackianus*, and *Potamogeton crispus*. This study focused on the five species that tend to accumulate on fine-particle screens, as shown in Figures 8–12 (*E. densa*, *E. nuttallii*, *H. verticillata*, *L. major*, and *V. asiatica*). *E. densa* was found to be distributed throughout the target channels, especially from the channel centers to downstream terminals. *E. nuttallii* was scattered and grew with slight coverage in the target channels. *H. verticillata* was distributed from the uppermost reaches to the centers of the target channels. We found more mixed communities with both *E. densa* and *V. asiatica* than communities with either of these species alone. While *L. major* grew locally between the upper terminals and centers of the target channels, no colonies of this species were observed, and only a few plants inhabited the channels in clusters. *V. asiatica* thrived throughout the entirety of the target channels. In the central target channel areas, some areas contained communities composed only of this species, but throughout the entire channels, we found many areas containing mixed communities of *V. asiatic* with *E. densa* and *P. malaianus*.

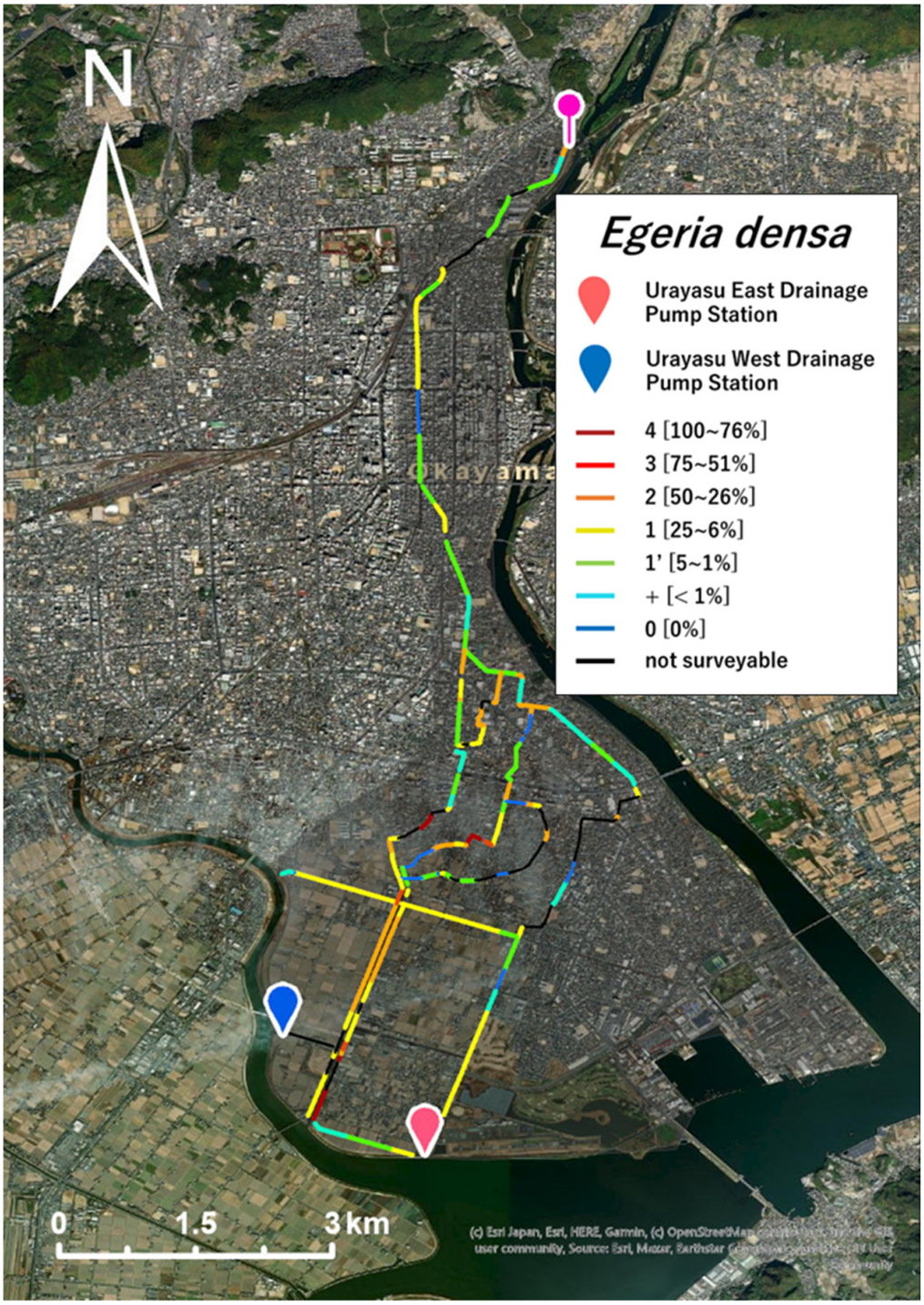

Figure 8. Map of the *E. densa* distribution. Copyright: Esri Japan, Esri, HERE, Garmin; OpenStreetMap contributors, and the GIS user community. Source: Esri, Maxar, Earthstar Geographics, and the GIS user community.

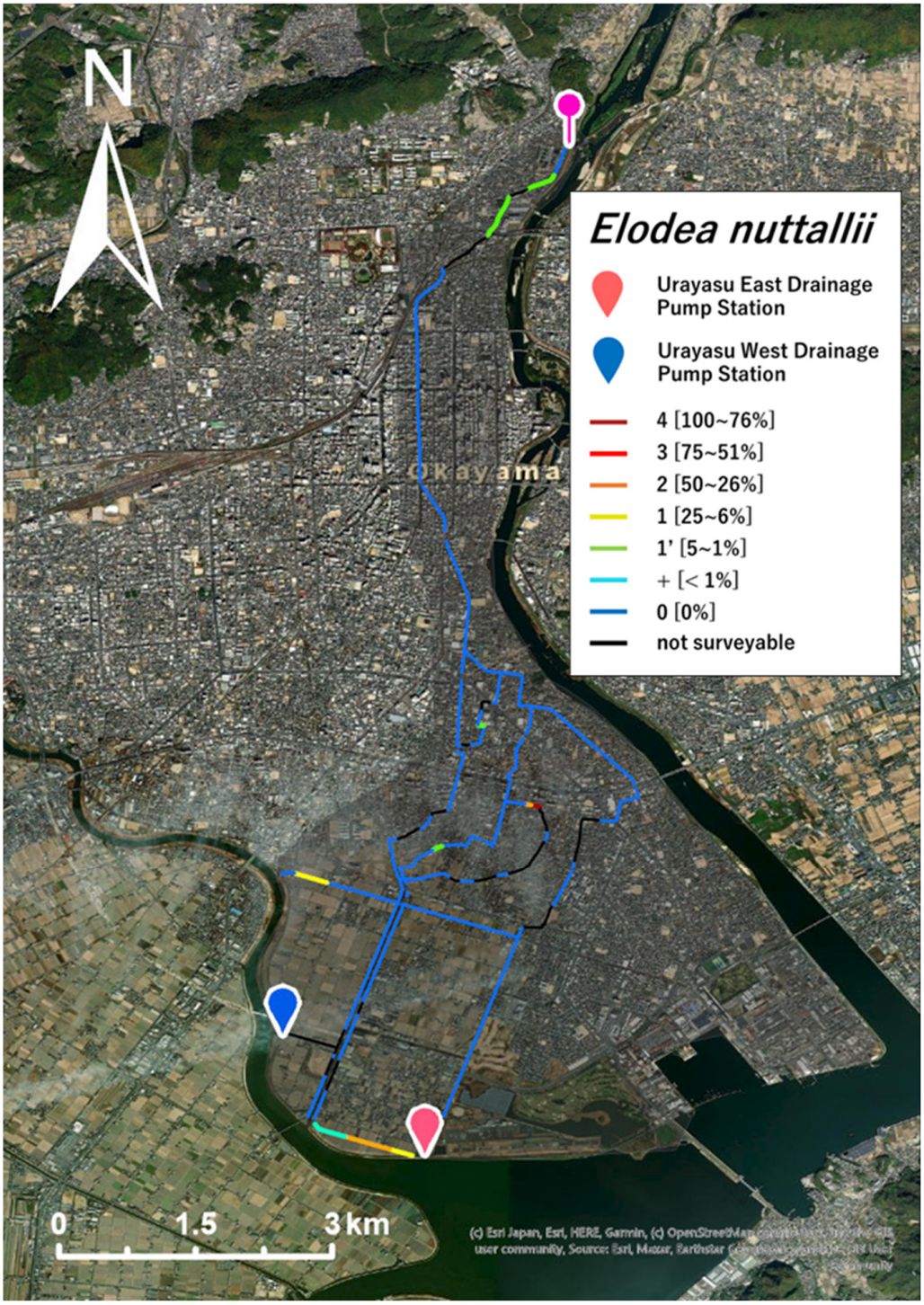

Figure 9. Map of the *E. nuttallii* distribution. Copyright: Esri Japan, Esri, HERE, Garmin; OpenStreetMap contributors, and the GIS user community. Source: Esri, Maxar, Earthstar Geographics, and the GIS user community.

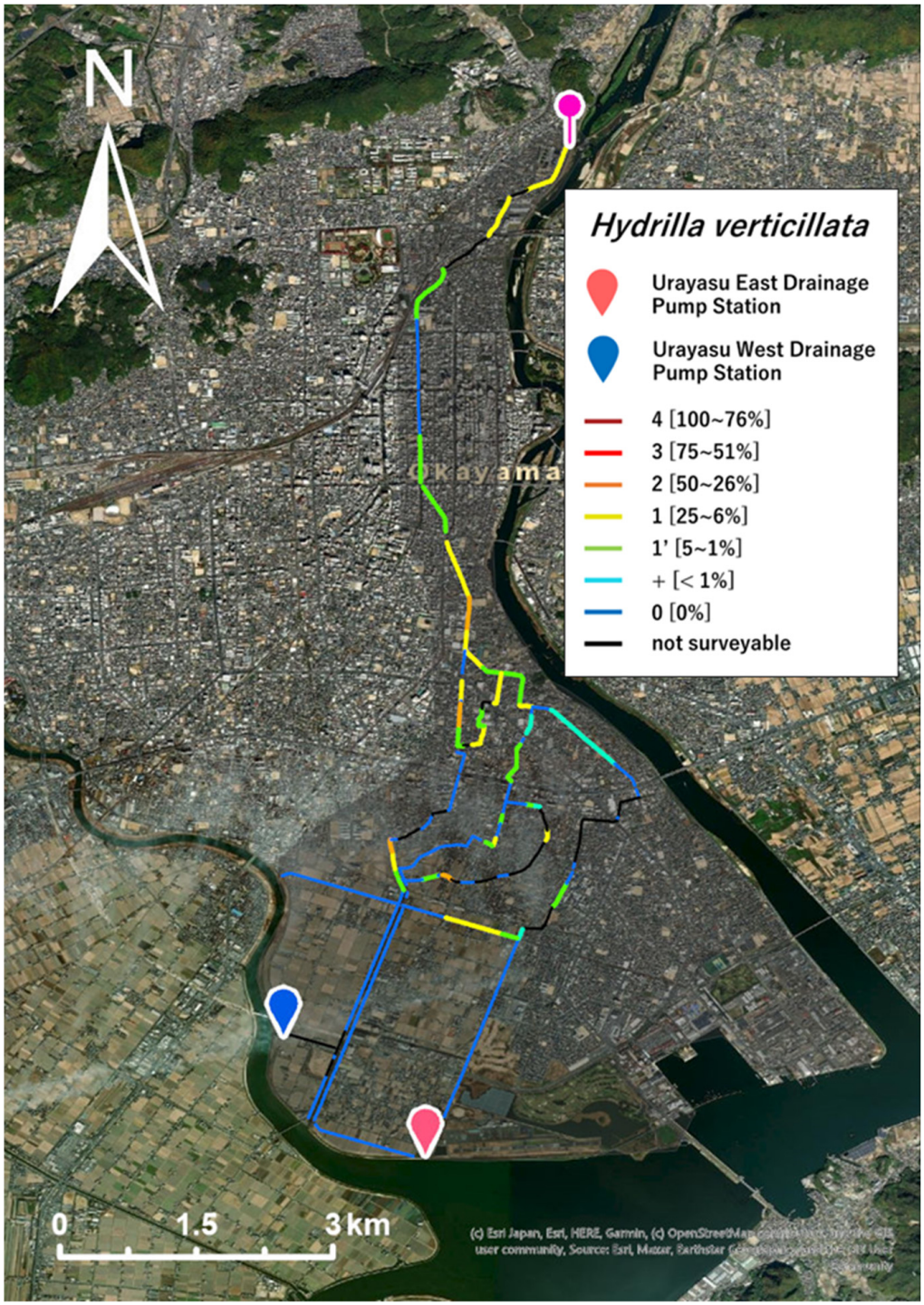

Figure 10. Map of the *H. verticillata* distribution. Copyright: Esri Japan, Esri, HERE, Garmin; OpenStreetMap contributors, and the GIS user community. Source: Esri, Maxar, Earthstar Geographics, and the GIS user community.

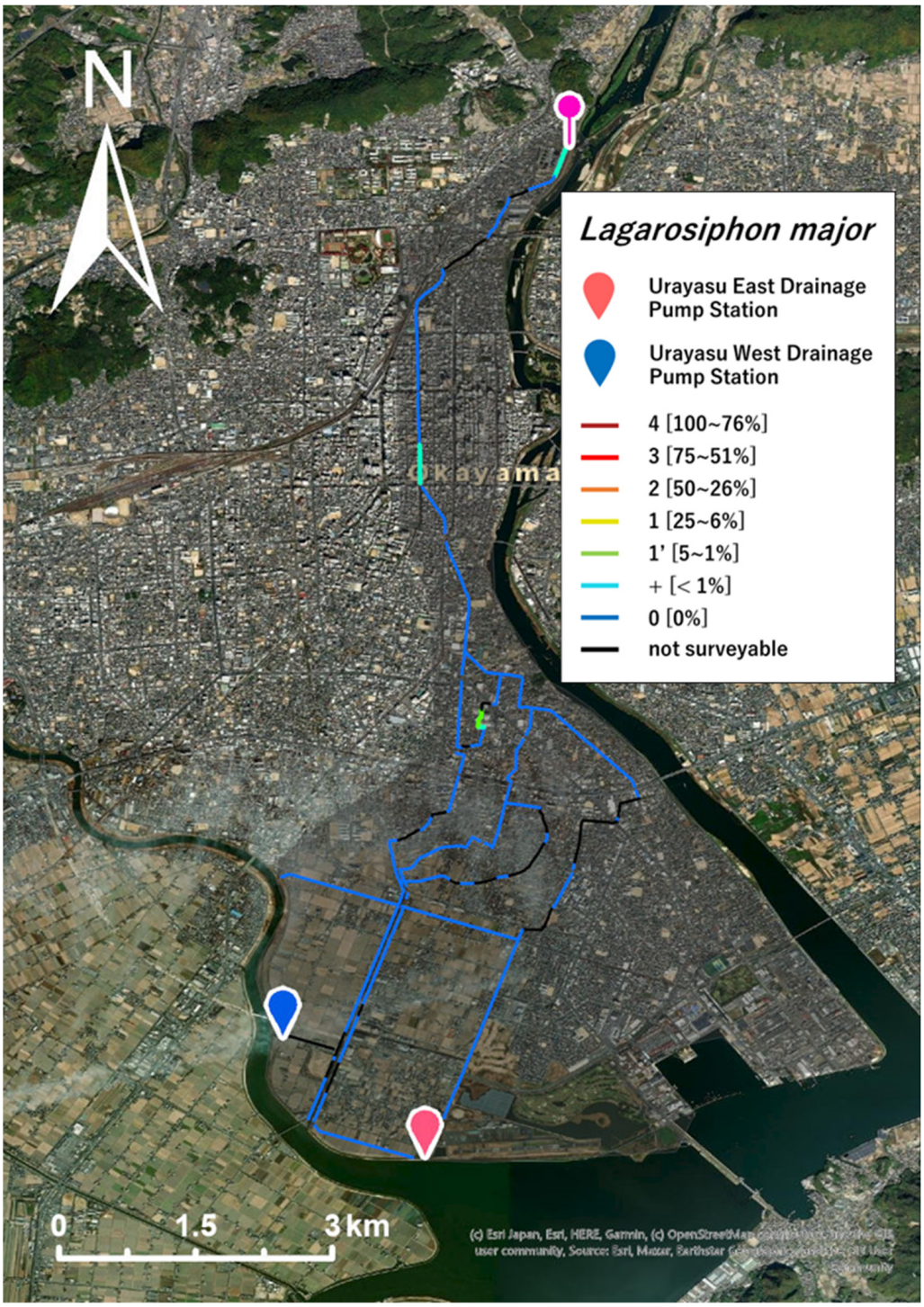

Figure 11. Map of the *L. major* distribution. Copyright: Esri Japan, Esri, HERE, Garmin; OpenStreetMap contributors, and the GIS user community. Source: Esri, Maxar, Earthstar Geographics, and the GIS user community.

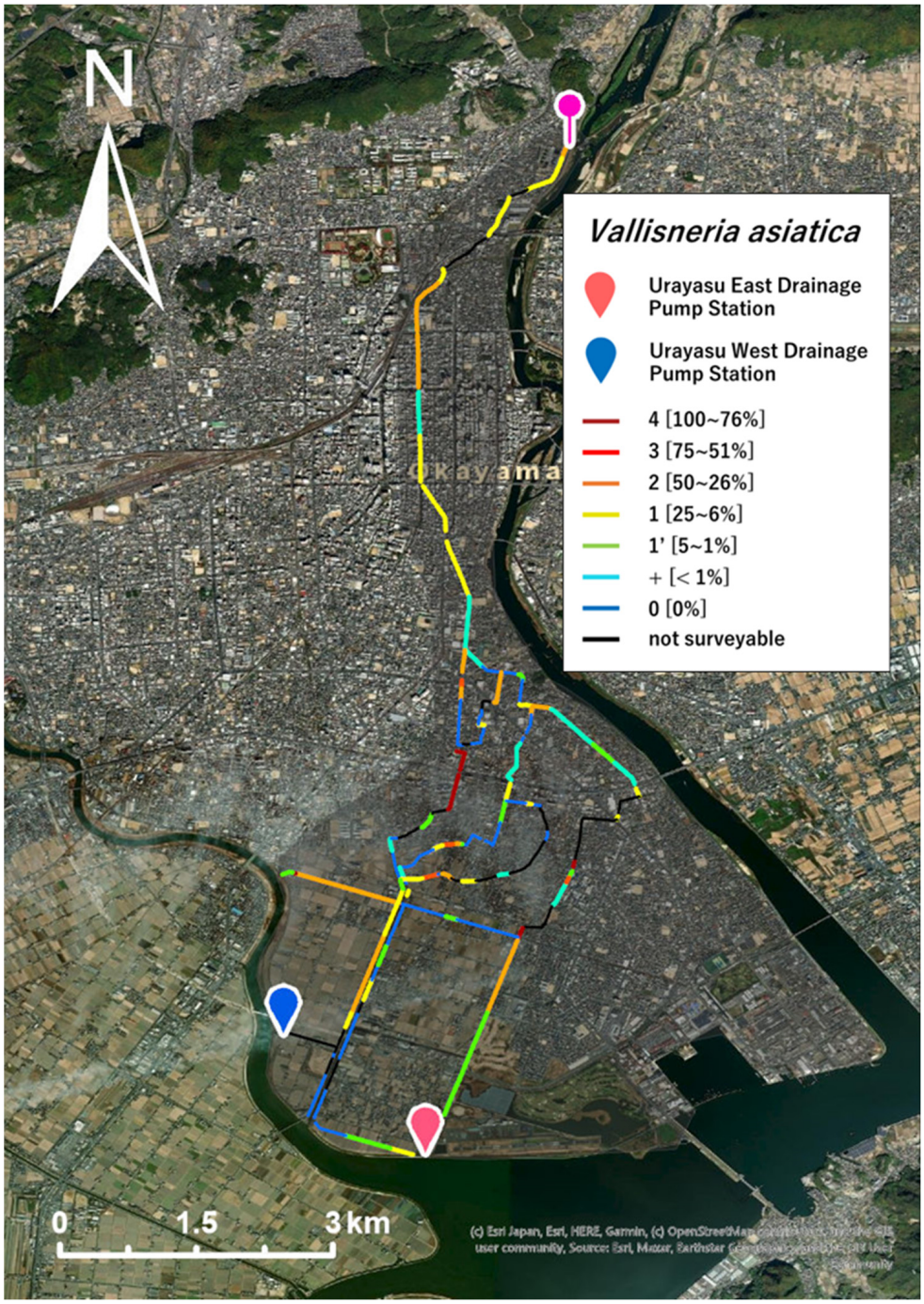

Figure 12. Map of the *V. asiatica* distribution. Copyright: Esri Japan, Esri, HERE, Garmin; OpenStreetMap contributors, and the GIS user community. Source: Esri, Maxar, Earthstar Geographics, and the GIS user community.

Based on the results of our distribution survey, we selected sections in which the aquatic plant species that easily accumulate on fine-particle screens were abundant and used these sections to determine priority control sections. The aquatic plant species that tend to accumulate on fine-particle screens were also found to thrive in the channels that flow into the Urayasu West Drainage Pump Station channel, where the water level simulations indicated an inland flooding risk resulting from backwater caused by aquatic plant-induced clogging. Therefore, it is necessary to select these channels as priority control sections. From the above information, we proposed the six locations shown in Figure 13 as priority control sections.

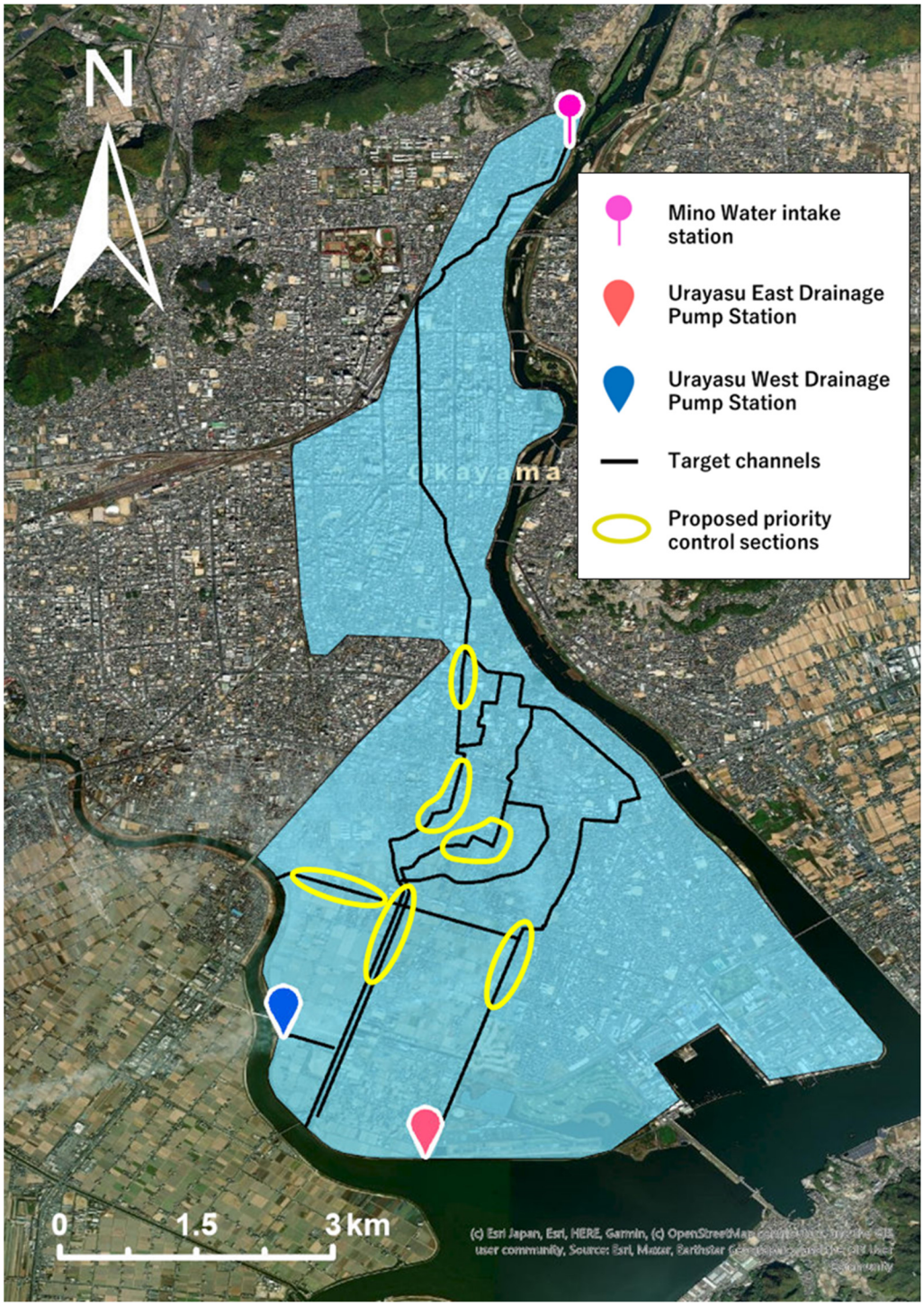

Figure 13. Proposed priority control sections. Copyright: Esri Japan, Esri, HERE, Garmin; OpenStreetMap contributors, and the GIS user community. Source: Esri, Maxar, Earthstar Geographics, and the GIS user community.

4. Conclusions

In this study, we evaluated the changes in the inland flooding risk posed by rising water levels resulting from the backwater caused by the clogging of fine-particle screens by aquatic plants. The simulation result of the Urayasu West Drainage Pump Station channel suggests that when the initial water depth is 70% of the channel depth and the discharge is 40 m^3/s in the Urayasu West Drainage Pump Station channel, inland flooding will not occur unless backwater occurs due to clogging by aquatic plants; however, inland flooding

will occur when backwater of 0.2 m or more occurs. Moreover, the discharge of 40 m^3/s is roughly equivalent to a rainfall intensity of 25–30 mm/h, and the results suggest a risk of inland flooding almost every year that backwater occurs in the Urayasu West Drainage Pump Station channel.

In addition, we proposed six priority control sections based on the results of an aquatic plant distribution survey. Because these are sections where aquatic plants that easily accumulate in fine-particle screens are particularly abundant, these sections should be intensively controlled to efficiently reduce the amount of aquatic plants. Considering that the abovementioned methods utilized in this study have not been used in previous studies and that water flow obstructions have been caused by the clogging of aquatic plants at drainage pump stations and places other than Okayama city, this study reveals the importance of conducting water level simulations and distribution surveys in areas other than Okayama city.

Future issues to be studied include the consideration of frictional energy losses due to the resistance of aquatic plant communities and conducting seasonal distribution surveys to gather more information on the plant species distributions and priority control areas. This subsequent work would be valuable because the abundances and locations of aquatic plant species fluctuate both seasonally and annually. In addition, we did not consider the difference in the erosion capacity between clean and sediment-laden waters. This is a subject for future analysis.

Author Contributions: Conceptualization, T.I. and K.T.; formal analysis, T.I.; investigation, T.I. and Y.N.; software, T.I. and K.T.; visualization, T.I.; writing—original draft, T.I.; writing—review and editing, T.I., K.T. and Y.N. All authors have read and agreed to the published version of the manuscript.

Funding: Part of this study is funded by JSPS KAKENHI JP 19KK0171, Okayama University Assignment of Research Support Staff, and Okayama University Return to Work Subsidy.

Data Availability Statement: Please contact the author to request data.

Acknowledgments: We thank the Okayama City Office for their administrative management while conducting field surveys. We are also grateful to Yasushi Mori of Okayama University for the valuable comments and to Ryo Nakaine, Yuta Matsuo, and Kesuke Nakamoto for helping us conduct the distribution survey.

Conflicts of Interest: The authors declare no conflict of interest.

References

1. IPCC. AR6 Climate Change 2021: The Physical Science Basis. Available online: https://www.ipcc.ch/report/sixth-assessment-report-working-group-i/ (accessed on 27 December 2021).
2. Japan Meteorological Agency. Past Changes in Heavy Rainfall and Extreme Heat Days (Extreme Phenomena). Available online: https://www.data.jma.go.jp/cpdinfo/extreme/extreme_p.html (accessed on 21 January 2022).
3. National Research Institute for Earth Science and Disaster Resilience. Basic Disaster Prevention Course, Basic Knowledge: 11. Inland Flooding. Available online: https://dil.bosai.go.jp/workshop/01kouza_kiso/11naisui.html (accessed on 10 January 2022).
4. Hirai, M.; Michiue, M.; Hinokidani, O. Modeling of flooding phenomenon in urbanized area. *Proc. Hydraul. Eng.* **1996**, *40*, 405–412. [CrossRef]
5. Okayama City. Okayama City Basic Plan for Flood Control 2019 Chapter 1: The Situation Surrounding Okayama City. Available online: https://www.city.okayama.jp/kurashi/cmsfiles/contents/0000017/17179/000309128.pdf (accessed on 23 June 2021).
6. Okayama City. Okayama City Action Plan for Flood Control 2019. Available online: https://www.city.okayama.jp/kurashi/cmsfiles/contents/0000017/17181/000367639.pdf (accessed on 24 June 2021).
7. Mineta, T. Waterweeds using agricultural water facilities (Symposium of Association of Japanese Agricultural Scientific Societies, Water and Agricultural Science). *Agric. Hortic.* **2021**, *96*, 96–97. (In Japanese)
8. Bates, R.P.; Hentges, J.F. Aquatic weeds—Eradicate or cultivate? *Econ. Bot.* **1976**, *30*, 39–50. [CrossRef]
9. Arif, A.S.M.; Uddin, M.S.; Islam, M.S.; Nusrat, S.; Das, P.R.; Biswas, M. Seasonal variation of aquatic weeds at *Dekar haor* under Sunamganj district, Bangladesh. *Fish. Aquat. Stud.* **2018**, *6*, 449–454.
10. Hassan, A.; Nawchoo, I.A. Impact of invasive plants in aquatic ecosystems. In *Bioremediation and Biotechnology: Sustainable Approaches to Pollution Degradation*; Hakeem, K.R., Bhat, R.A., Qadri, H., Eds.; Springer International Publishing: Cham, Switzerland, 2020; pp. 55–73.
11. Narayan, S.; Nabi, A.; Hussain, K.; Khan, F. *Practical Aspects of Utilizing Aquatic Weeds in Compost Preparation*; 2017. [CrossRef]

12. Bornette, G.; Amoros, C.; Lamouroux, N. Aquatic plant diversity in riverine wetlands: The role of connectivity. *Freshw. Biol.* **1998**, *39*, 267–283. [CrossRef]
13. Kawaike, K.; Inoue, K.; Toda, K.; Noguchi, M. Inundation flow analysis due to heavy rainfall in low-lying urbanized river basin. *Jpn. Soc. Civ. Eng.* **2004**, *2004*, 57–68. [CrossRef]
14. Sekine, M. Numerical analysis of inundation in the region of downtown Tokyo with residence area. *J. Jpn. Soc. Civ. Eng. B1 Hydraul. Eng.* **2011**, *67*, 70–85. [CrossRef]
15. Djamres, E.K.D.; Komori, D.; Kazama, S. Topographical characteristics of frequent inland water flooding areas in Tangerang City, Indonesia. *Front. Water* **2021**, *3*, 661299. [CrossRef]
16. Nakaguchi, K.; Inomata, R.; Komori, D. *Spatial Distribution of Inland Flooding Risk and Its Factors in Japanese Cities*; Japan society of Hydrology and Water Resources: Tokyo, Japan, 2019. (In Japanese) [CrossRef]
17. Kinki Regional Development Bureau; Ministry of Land, Infrastructure, Transport and Tourism. Chapter 4 Drainage. Available online: https://www.kkr.mlit.go.jp/plan/jigyousya/technical_information/consultant/binran/etsuran/qgl8vl0000005ecr-att/sekkei03_04.pdf (accessed on 25 January 2022).
18. Nakatsugawa, M.; Shimizu, Y. *Hydraulics for Practical Fields (1)—Calculation of Unequal Flow in Single Cross-Sections*; Civil Engineering Research Institute for Cold Region: Sapporo, Japan, 1987; pp. 1–5. Available online: https://river.ceri.go.jp/contents/uploads/docs/suirigaku_old01.pdf (accessed on 12 May 2022). (In Japanese)
19. Weed Science Society of Japan. Method in weed science. *Weed Sci. Soc. Jpn.* **2001**, 65–66. (In Japanese)
20. Japan Meteorological Agency. Historical Weather Data Search. Available online: http://www.data.jma.go.jp/obd/stats/etrn/index.php?prec_no=66&block_no=47768&year=&month=&day=&view=h0 (accessed on 2 February 2022).
21. Okayama City. Okayama City Map Information. Available online: http://www.gis.pref.okayama.jp/okayamacity/Map?mid=1070&mpx=133.9181064647889&mpy=34.596556122583166&mps=10000&mtp=r_dm&gprj=3&mcl=80031,1,10,100;80031,2,20,200;80031,3,30,300;80031,4,40,400 (accessed on 12 May 2022).